Fast estimation of the derailment risk of a braking train in curves and turnouts

Burgelman, Nico; Li, Zili; Dollevoet, Rolf

DOI
10.1504/IJHVS.2016.077320

Publication date
2016

Document Version
Accepted author manuscript

Published in
International Journal of Heavy Vehicle Systems

Fast Estimation of the Derailment Risk of a Braking Train in Curves and Turnouts

Nico Burgelman*, Zili Li and Rolf Dollevoet

Faculty of Civil Engineering and Geosciences,
Delft University of Technology
Postbus 5048, 2600GA
Delft, the Netherlands
E-mail: n.d.m.burgelman@tudelft.nl
E-mail: z.li@tudelft.nl
E-mail: r.p.b.j.dollevoet@tudelft.nl
*Corresponding author

Abstract When a train runs through a turnout or a sharp curve, high lateral forces occur between the wheels and rails. These lateral forces increase when the couplers between the wagons are loaded in compression, i.e., a rear locomotive pushing a train or a front locomotive braking a train. This study quantifies these effects for a train that begins braking when steadily curving and for a train that brakes upon entering a turnout. Our approach allows distinguishing between the effects of braking and the transient effects of entering the turnout. The dynamic derailment quotient is mapped as a function of the vehicle speed and the braking effort. Then the dynamic derailment coefficient obtained from the dynamic simulations are compared to results from quasi statics. This allows determining a dynamic multiplication coefficient that can be used on the quasi static derailment coefficient to obtain a first estimate of the dynamic derailment coefficient.

Keywords: longitudinal train dynamics; turnout; derailment quotient; vehicle simulation; braking

Biographical notes: Nico Burgelman received a M.Sc. in Electromechanical Engineering from the University of Ghent in 2007, and M.Sc. in Applied Mechanics from Chalmers University of Technology in 2010. He finished his PhD at Delft University of Technology in 2015. He is currently working for DEKRA Rail as a specialist in railway mechanics. His research interests include railway vehicle dynamics, track monitoring and wheel-rail contact mechanics.

Dr. Zili Li received the B.Sc. and M.Sc. degrees in mechanical engineering from Southwest Jiaotong University, Chengdu, China, in 1988 and 1991, respectively. He received the PhD degree from Delft University of Technology, Delft, The Netherlands, in 2002. Between 1999 and 2005 he was with the Institute of Road Transportation of TNO, Delft. He is currently an Associate Professor with the Section of Road and Railway Engineering, Delft University of Technology. His research interests include numerical solution of frictional rolling contact and its applications; train-track interaction, particularly in the high-frequency; condition monitoring of tracks.

Prof. Rolf Dollevoet received the M.Sc. degree in mechanical engineering from Eindhoven University of Technology, Eindhoven, The Netherlands, and the PhD. degree from the University of Twente, Enschede, the Netherlands, in 2010. Since 2003 he has been with ProRail, Utrecht, the Netherlands. Since 2012, he has

been appointed as a part-time Professor with the Section of Road and Railway Engineering, Delft University of Technology, Delft, The Netherlands.
This paper is a revised and expanded version of a paper entitled *Some Preliminary Results in Simulation of Interaction between a Pushed Train and a Turnout* presented at the 22nd International Symposium on Dynamics of Vehicles on Roads and Tracks, Manchester, UK (August 15-19, 2011).

1 Introduction

1.1 Background on longitudinal-lateral train dynamics.

The effects of braking and traction on long trains have often been studied from the longitudinal dynamics point of view [1]. The longitudinal problem can be solved with just one degree of freedom per vehicle, thereby limiting the calculation effort even for long trains. Many authors have published longitudinal coupler models that include non-linear springs, slack and/or friction [2, 3, 4, 5, 6]. Others have studied the combination of the longitudinal and vertical problems [7] including the wheel unloading due to bogie or carbody pitch and bounce. The pitch and bounce modes are excited because the centers of gravity of the vehicles are often higher than the couplers, particularly when the wagons are loaded [1]. The lateral forces in long trains were first studied by El-Sibaie [8], who conducted an experimental analysis of the problem. The lateral coupler forces on one test wagon were controlled by actuators on the adjacent vehicle; then, the train ran through a curve, while the forces on the wheels were measured using an instrumented wheelset. This approach allows monitoring of the relationship between vehicle speed and coupler force, and the derailment quotient. Cole et al. [9] (amongst others) combined simulations of longitudinal train dynamics with quasi-statics to obtain the lateral forces; the coupler angles were calculated using an approach suggested by [10]. Xu et al. [11, 12] combined a detailed model of three vehicles with a simple model (1 degree of freedom) for most vehicles; this approach reduced the total degrees of freedom and so the calculation effort. The vehicles modeled in detail were the locomotives and the adjacent wagons because it is between them that the highest coupler forces occur. They concluded that the rotation limit for the coupler best be set to 4°.

This paper features simulations of a train consisting of a locomotive followed by seven wagons, each of which is modeled with 42 degrees of freedom, thus including all lateral, vertical and longitudinal motions and rotations. The model is of a passenger train; therefore the secondary suspension is soft compared to freight vehicles, and the results obtained are useful for operators of passenger trains. This work could be particularly applicable in designing pulling/pushing policies for passenger trains in shunting yards. Shunting yards have many turnouts, that often receive insufficient maintenance; therefore most derailments happen there. Although the paper does not address long freight trains, our methodology and estimation/mapping could be useful for heavy-haul operators.

1.2 Background on vehicle-turnout interaction

The interactions between trains and tracks are most violent at turnouts due to the complex geometry and structure. Improperly designed or maintained turnouts can cause discomfort

to passengers, damage to cargo, or even a derailment. Maintenance and repair of turnouts are a major cost driver for many infrastructure managers.

Lateral train-track interaction force is high in turnouts due to their small curve radii, and it might be increased further by the compressive forces in the couplers of a train due to braking or traction. A high lateral force may lead to deformation of the control mechanism of a switch, and a lateral shift of the entire track. A deformed stretch bar of the control mechanism may lead to incorrect positioning of switch blades. All of these may result in malfunctioning of turnouts, causing wheel climb and subsequent derailment. Wear and head checking are other common consequences of high wheel-rail contact forces.

There are many aspects to the modeling of vehicle-turnout interactions, and different authors have focused on different aspects. Menssen and Kik [13] were among the first to address the numerical simulation of a rail vehicle passing through a turnout. Some of the most recent work in vehicle-turnout interaction has been performed by Kassa and Nielsen [14] and Alfi and Bruni [15]. They focused on the detailed modeling of a single vehicle passing a turnout, with flexibilities to account for high frequency phenomena. Other authors have focused on the wheel-rail contact in turnouts, which is complex due to the profiles of the switch blade and the crossing. Wiest et al. [16] and Shu et al. [17] focused on the normal contact problem, while Burgelman et al. [18] considered the tangential problem. To the authors' knowledge, all the models in the literature to date have included a single vehicle coasting through a turnout. Work on train-turnout interaction rather than vehicle-turnout interaction appears lacking, particularly analysis of the influence of the coupler forces on the lateral train dynamics and on the derailment quotient.

The goals of this paper are to establish a simple method to quickly assess the derailment risk by estimating the derailment quotient, and to validate this method using vehicle dynamic simulations with a detailed model of a locomotive followed by seven wagons. To this end, quasi-statics is used to obtain a first guess of the derailment quotient. Because quasi-statics does not require any simulation, this can be performed easily for any combination of curve radius, braking force, number of vehicles, etc. Then, simulations are performed to calculate the maximum derailment quotient of a locomotive followed by seven wagons on a curve or a turnout. This dynamic derailment quotient is used to define a dynamic multiplication coefficient to be used with the static derailment quotient. Mapping the derailment quotient as function of speed and braking effort can provide a tool to train operators formulate upon their braking protocols. Assessing the derailment risk without long and complex vehicle simulations might be especially interesting when a fast estimate is required for a train configuration different from those in typical daily operations.

Relating the results from quasi-static calculation with measured or simulated results in order to obtain a fast way of estimating the dynamic forces has been investigated before. The dynamic wheel-rail forces on curves and straight track including track irregularities have been mapped in [19] based on results from [20] and [21]. Grassie [22] published a relation between the quasi-static load and the dynamic vertical track forces as a transfer function which is basically a wavelength-depended multiplication factor. Dietrich et al. [23] have investigated the effect of cross wind; they concluded that the allowable cross wind was just $3\,\mathrm{m/s}$ lower when calculated with quasi-statics compared to calculated using a vehicle dynamic simulation.

the assumptions made in the quasi-static analysis are violated in reality, but the results will still be valid, as long as it is possible to define a dynamic multiplication coefficient which allows obtaining a reasonable estimate of the dynamic force in a usable range of vehicle speeds and traction/braking efforts. This means that all contributions to the dynamic lateral

force that scale approximately linearly with the traction/braking effort and quadratically with the vehicle speed are accounted for.

2 The model

2.1 Track model

Two models are used: one for a curved track with a transition and one for a turnout without a transition. The curve is modelled with the same radius as the turnout: $260\,\mathrm{m}$ and without cant. This way we can analyse separately the transient responses from braking and from entering the turnout. In reality, a curve will; always have a certain cant except for some trams that share the tramway with road vehicles. The diverging route was modelled, meaning that there is no transition curve between the straight track and the curvature of the turnout. The rail profiles used for the tong of the turnout were obtained through measurements on a 1:9 turnout, which had been in regular service for some years [24]. This turnout was described as heavily worn and was on the limit of the safety criteria for profile change.

2.2 Vehicle model

The vehicles modeled are those of the VIRM trains of the Dutch Railways. Each vehicle has 42 degrees of freedom (dof): 6 dof for each of the wheelsets, the bogie frames and the carbody. All major nonlinearities in the primary and secondary suspension are considered, including the friction dampers, the bump stops and the airsprings. The model has been validated by comparing the hunting wavelength obtained from simulations with wavelengths observed from wear patterns on the rails [25]. The wheel-rail contact was treated using the multi-Hertzian approach for the normal contact problem and the FASTSIM algorithm for the tangential contact problem.

2.3 Train configuration

The configuration of the train is shown in Figure 1. The passage of a locomotive followed by 7 identical wagons is simulated through a curve and a turnout. A braking force is applied to the wheels of the locomotive when the first wagon enters the turnout, which is implemented in the model as an actuator applying a moment between the axle boxes and the wheelsets. The wheelsets of the wagons do not apply traction or braking. The train is modelled with of 336 degrees of freedom (8x42). For the simulations in this article, with a simulation times from $5\,\mathrm{s}$ to $10\,\mathrm{s}$, the computation time was found to be around $10\,\mathrm{min}$ on a common computer.

2.4 Coupling of the coaches

The VIRM vehicles are coupled with Scharfenberg couplers. This type of coupler does not transfer any yaw moment when coupler angles are small. It is modeled as one spring in parallel with a damper, positioned in the center-line of the vehicles; the force-displacement curves of the non-linear springs have been obtained from [2]. Buffers and chain couplers, used mostly in freight vehicles, consist of a center chain that transfers the pulling forces and one buffer on each side, transferring pushing forces. The buffers and chain coupler are modeled as two spring/damper pairs, one on each side. This type of coupler transfers a yaw moment between the carbodies.

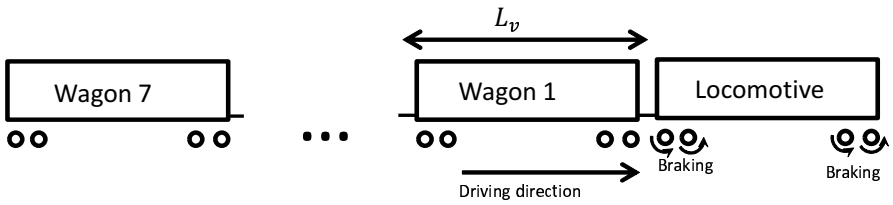

Figure 1 Overview of the train and the applied traction and braking.

2.5 Quasi-static derailment quotient

If all energy dissipation from wheel-rail contact, the suspension elements and air resistance is neglected, the effect of braking is to consume the kinetic energy of the train and dissipate it in the brakes. Because all the vehicles are subject to the same deceleration, the force in each coupler is proportional to the total mass of the vehicles behind it. Therefore, the coupler forces will be largest in the coupling between the locomotive and the first wagon:

$$F_{c1} = \frac{7m_{\mathrm{wag}}}{7m_{\mathrm{wag}} + m_{\mathrm{loc}}} F_{\mathrm{braking}} \tag{1}$$

with

$$F_{\mathrm{braking}} = \mu\, g\, m_{\mathrm{loc}} \tag{2}$$

where μ is the braking coefficient defined as the braking force per wheelset divided by the axle load, g is the gravity constant, m_{loc} is the mass of the locomotive (here $88\,000\,\mathrm{kg}$), m_{wag} is the mass of a wagon (here $80\,000\,\mathrm{kg}$), F_{braking} is the total braking force applied by the locomotive, and F_{c1} is the force in the first coupler.

Because the coupling does not transfer a yaw moment, the resultant force of the coupler on a wagon is always in the direction of the coupler. Define ϕ as the coupler angle, i.e., the angle between the coupler and the vehicle (see Section 2.6); the lateral component of the coupler force becomes:

$$F_{\mathrm{lat}c1} = F_{c1} \sin\phi \tag{3}$$

This lateral force is distributed among the wheelsets of the vehicle. Assuming that these forces are distributed uniformly by the wheelsets of the bogies adjacent to the coupler (because the other bogie must carry the lateral force introduced by the other coupler) and assuming that the lateral load due to the centripetal force is uniformly distributed, the lateral force, Y, per wheelset on the wheelsets of the leading bogie of the first wagon becomes:

$$Y = \frac{F_{c1}\sin\phi}{2} + \frac{m_{\mathrm{wag}}}{4}\left(\frac{V^2}{R} - g\epsilon\right) \tag{4}$$

where V is the velocity of the train, ϵ is the cant angle, and R is the curve radius. The derailment quotient is the ratio of the lateral force to the vertical force, Q, of the outer wheel in the turnout. If we assume that the lateral force is transferred to the track by the outer

wheel and neglect the lateral force on the inner wheel, the lateral force on the outer wheel is Y. The vertical force on the outer wheel can be estimated by quasi-statics as follows:

$$Q = \frac{m_{\mathrm{wag}}}{8} g + \frac{m_{\mathrm{wag}}}{4} \left(\frac{V^2}{R} - g\epsilon \right) \frac{h}{l} \tag{5}$$

where h is the height of the center of gravity of the vehicle above the rail top, and l is the track width.

2.6 Coupler angle calculation

The magnitude of the coupler angle affects the lateral component of the coupler forces. Simson [10] has proposed an approach to calculate the coupler angle that can be extended for a transition curve or a turnout. If we ignore the displacements in the bogie suspension and the stiffness of the coupler, then the bogie pivot center is located above the center of the track, and the coupler has a fixed length. Hence the coupler angle becomes independent of forces and velocities and depends only on geometric variables: dimensions of the vehicles (the distance between the bogies, the distance between the bogie and the coupler pivot and the length of the coupler itself) and the track curvature. In the case of a curve transition or a turnout, the local track curvature needs to be known at each point of the track where the two vehicles adjacent to the coupler are. The general case is shown in Figure 2

$$L = B_i + B_{i+1} + D \tag{6}$$

where L is the distance between the centers of the two bogies of adjacent vehicles (assuming small angles), B_i and B_{i+1} are the overhangs, i.e., the distances between the centers of the bogies and the pivots of the coupler link, and D is the distance between the two coupler pivots.

The angle between the carbodies of the two vehicles, θ, can be calculated as follows:

$$\theta = \alpha + \beta + 2\gamma \tag{7}$$

where α and β are the angles between each vehicle and the tangent to the track in the bogie pivot adjacent to the coupler (i.e., points r_i and f_{i+1}, see Figure 2) and γ is the angle between the two tangents to the track in r_i and f_{i+1}. These angles can be calculated using integrals along the track ($\mathrm{d}s$):

$$\alpha = \frac{1}{2A_i} \int_{r_i}^{f_i} \int_{r_i}^{s} \frac{1}{R_{\mathrm{local}}} \,\mathrm{d}s \,\mathrm{d}s \tag{8}$$

$$\beta = \frac{1}{2A_{i+1}} \int_{f_{i+1}}^{r_{i+1}} \int_{f_{i+1}}^{s} \frac{1}{R_{\mathrm{local}}} \,\mathrm{d}s \,\mathrm{d}s \tag{9}$$

$$\gamma = \frac{1}{2} \int_{f_{i+1}}^{r_i} \frac{1}{R_{\mathrm{local}}} \,\mathrm{d}s \tag{10}$$

where A_i is half the distance between the two bogie pivots of vehicle i.

If the curve radius is piecewise constant between the bogie pivots then α, β and γ can be calculated as:

$$\alpha = \frac{A_i}{R_i}\,, \qquad \beta = \frac{A_{i+1}}{R_{i+1}}\,, \qquad \gamma = \frac{L}{2R_l} \tag{11}$$

where R_i is the curve radius between f_i and r_i, and R_l is the radius between f_{i+1} and r_i.

The coupler angles (see [10]) are the angles between the coupler and vehicle i, ϕ_i, or vehicle $i+1$, ϕ_{i+1}:

$$\phi_i = \frac{L(\gamma+\alpha) - B_{i+1}\theta}{D}\,, \qquad \phi_{i+1} = \frac{L(\gamma+\beta) - B_i\theta}{D} \tag{12}$$

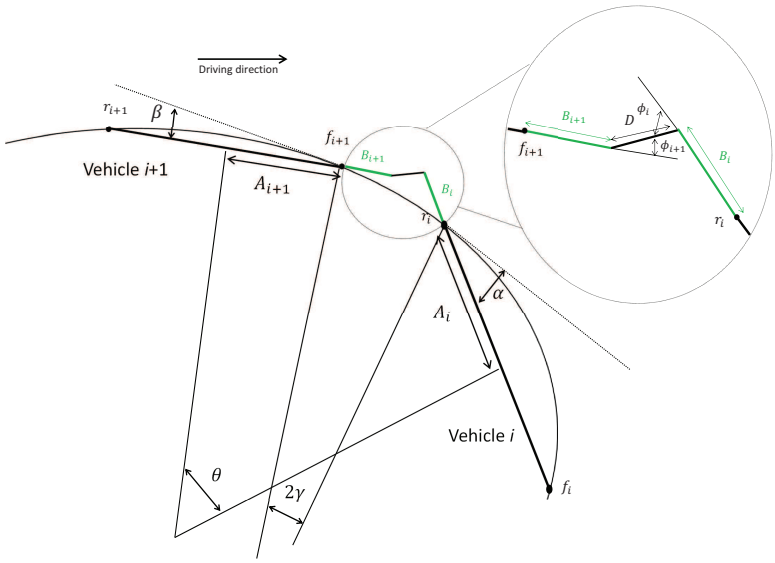

Figure 2 The coupler angle in a curve with varying radius.

2.7 Coupler angle in a curve and upon entering the turnout

For a curve with constant radius R and two geometrically identical vehicles, the angle a coupler makes with the centerlines of the wagons to which it is attached is: $\phi = \frac{L_v}{2R}$, where L_v is the length of one wagon including the couplers (see Figure 1). This equation is a simplification of equation (12); the two coupler angles are identical and depends only on the total vehicle length and the curve radius. For the vehicle in this study and a $260\,\mathrm{m}$ curve, the resulting coupler angle is $2.75°$. Connecting two vehicles with a different geometry would result in a larger coupler angle.

A turnout consists of a straight part followed, without transition, by a curve with a constant radius. Therefore it is not necessary to evaluate the integrals of equations (8-10); equation 11 can be used instead. When a train passes a 1:9 turnout, the largest coupler angle occurs upon entering the turnout when the first vehicle is in the turnout ($R_1 = 260\,\mathrm{m}$) and the two bogies of the second vehicle are still on the tangent track ($R_2 = \infty$), while the overhang of the second vehicle is already in the turnout ($R_l = 260\,\mathrm{m}$); this situation is drawn in Figure 3. The resulting maximum coupler angle for the case study of this paper is $7.14°$ between the locomotive and the coupler; the angle between the coupler and the first wagon is smaller and acts in the other direction; i.e., the resulting lateral force from braking pushes the wagon inwards. Due to symmetry, a reverse situation will exist upon leaving the turnout, but the lateral force will be smaller because the quasi-static lateral force on the locomotive will be zero. Therefore this study focuses only on entering of turnout.

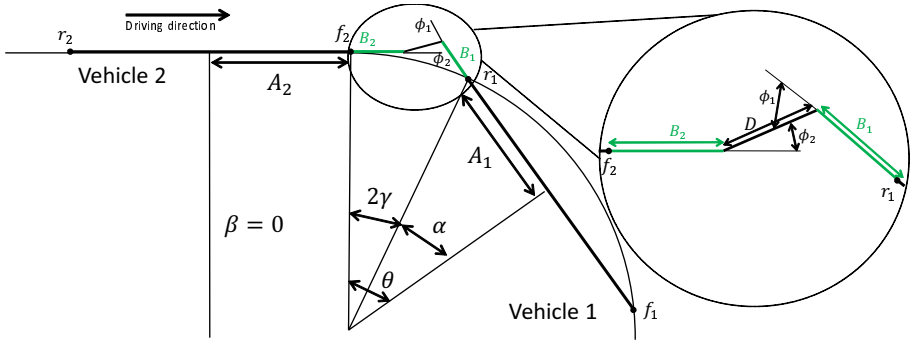

Figure 3 The coupler angle with vehicle 1 in the turnout and vehicle 2 with the leading bogie just at the beginning of the turnout.

3 Results

3.1 Quasi-statics

3.1.1 Curving

The derailment quotients calculated from equations (4) and (5) are plotted in Figure 4a as functions of the train velocity and the braking coefficient applied by the locomotive. The influence of the train velocity is larger than that of the braking; however the latter is not insignificant. A train entering a turnout at $40\,\mathrm{km/h}$, the maximum allowed speed in a 1:9 turnout, with the highest possible braking of the locomotive (i.e. braking coefficient = 0.6) creates a higher derailment quotient on the wheel than a train coasting (braking coefficient = 0) through the same turnout at $55\,\mathrm{km/h}$.

3.1.2 Turnout

In a turnout the coupler angle is much larger; therefore, compared to a curve the influence of the braking coefficient on the derailment quotient is also much larger. The derailment

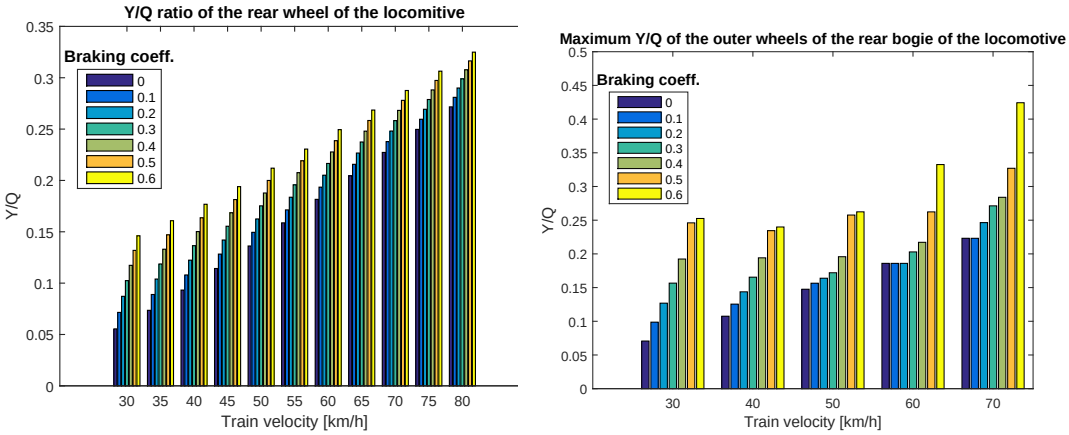

(a) (b)

Figure 4 The maximum derailment quotient of the outer wheels of the rear bogie of the locomotive in a curve, (a) calculated with equations (4) and (5), (b) obtained from dynamic simulations. The braking coefficient, ranges from 0 (no braking) to 0.6 (only achievable on dry track/perfect conditions). The velocity is swept from $30\,\mathrm{km/h}$ to $80\,\mathrm{km/h}$; $40\,\mathrm{km/h}$ is the maximum speed allowed in a 1:9 turnout.

quotient is shown in Figure 5a. The quasi-static derailment quotient of a train entering a turnout at $40\,\mathrm{km/h}$, the maximum allowed speed in such a turnout, surpasses the derailment quotient of a train running through the turnout at $80\,\mathrm{km/h}$ with a moderate braking coefficient of 0.2.

3.2 The vehicle eigenmodes

To understand the dynamic behavior of the train, a rigid body modal analysis was performed for a train with Scharfenberg couplers and a train with buffer-and-chain couplers (see Table 1). Most of the eigenmodes are identical except for the carbody sway, roll and yaw modes, where the yaw moment between the carbodies transferred by the couplers plays a role. Because of the yaw stiffness between the carbodies, the motions of the vehicles influence one another; therefore there is a range of frequencies for the carbody yaw and sway modes rather than one specific frequency. This range represents a number of closely related eigenmodes in which the adjacent vehicles move in phase or in anti-phase.

In the longitudinal carbody modes the train acts as a number of masses in series connected with springs. One can see this eigenmode as a standing longitudinal wave in the train. In the case of a discrete number of masses in series, the eigenfrequencies are close to multiples of the first standing wave. Unlike the other eigenmodes, which depend mostly on the vehicle properties, the longitudinal eigenmodes strongly depend on the train configuration, i.e., the number of vehicles; when the train is longer the eigenfrequency of the first longitudinal carbody mode will decrease in proportion to the number of vehicles.

3.3 Train simulations

The quasi-statics do not include some 'quasi statics' effects such as wheel unloading due to static carbody pitch. The static carbody pitch originates from the coupler forces that

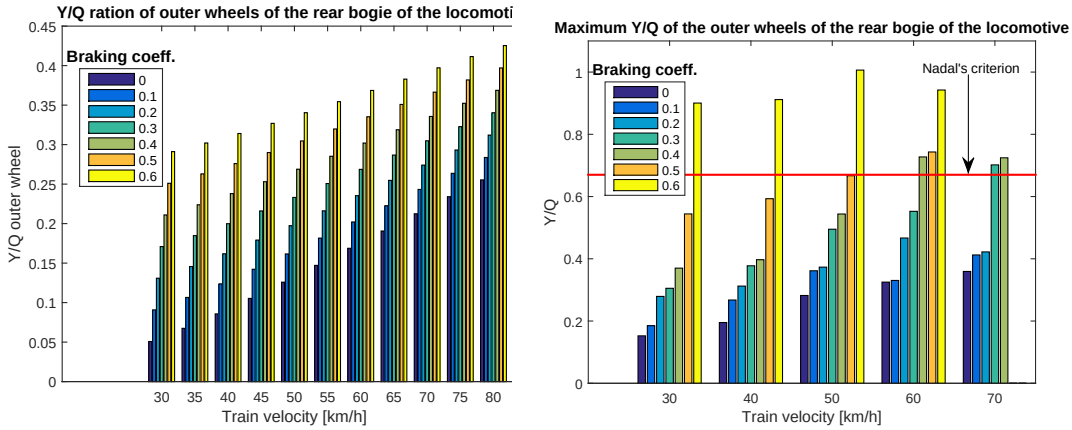

(a) (b)

Figure 5 The maximum derailment quotient of the outer wheels of the rear bogie of the locomotive in a 1:9 turnout, (a) calculated with equations (4), (5) and (12), (b) obtained from dynamic simulations. The braking coefficient ranges from 0 (no braking) to 0.6 (only achievable on dry track/perfect conditions). The velocity is swept from $30\,\mathrm{km/h}$ to $80\,\mathrm{km/h}$; $40\,\mathrm{km/h}$ is the maximum allowed speed in a 1:9 turnout. The horizontal line is the maximum derailment quotient according to Nadal (calculated with flange angle $65°$, and friction coefficient 0.6.)

Table 1 The eigenmodes and eigenfrequencies of the whole train model.

Eigenmode	Frequency in Hz	
	Scharfenberg	buffer-and-chain
Carbody sway of the wagons	0.42	0.36-0.37
Carbody sway of the locomotive	0.48	0.37
Carbody roll of the wagons	0.67-0.68	0.62
Carbody bounce of the wagons	0.79	0.79
Carbody bounce of the locomotive	0.84	0.84
Carbody yaw of the wagons	0.84	0.84-0.89
Carbody pitch of the wagons	1.1-1.2	1.1-1.2
Carbody pitch of the locomotive	1.2	1.2
Carbody longitudinal through the couplers	2.4-4.7-6.8-8.7	2.4-4.7-6.8-8.7
Bogie pitch of the wagons	5.9	5.9
Bogie roll of the wagons	9.3	9.3
Bogie higher modes	>10	>10

are not the same height above the rail as the center of mass of the vehicles; moreover, the locomotive static carbody pitch also originates from the braking forces on the wheels. To quantify the effects of the quasi-static assumption, a number of dynamic simulations were performed for two cases: first, a train steadily curving and then suddenly applying a braking force (Section 3.3.1), and second, a train braking upon entering a turnout (Section 3.3.2). Each case was simulated with 7 different coefficients of braking and 5 different initial train speeds.

The cases of a curve and a turnout allow studying the different dynamic effects, which are composed of the eigenmodes of the train. These dynamic effects can be split into two parts: first the dynamic effect due to application of braking, which changes the longitudinal acceleration of the vehicles, and second, the dynamic effect due to the curve transition, which changes the lateral acceleration of the vehicles.

3.3.1 Derailment quotient while curving

To study the influence of the dynamics in a turnout we have simulated the case of a train running at $40\,\mathrm{km/h}$ through a $260\,\mathrm{m}$ curve (see Figure 6). After the transient phenomena from entering the curve have died out, braking is applied to the wheels of the locomotive. Prior to braking, the wheels of the leading bogie of the first wagon carry the lateral load due to the centripetal force. The average of the force can be calculated from equation (4), but it is non-uniformly distributed in that the outer front wheel carries a much higher load than the outer rear wheel. The average lateral force from the simulation is $9.5\,\mathrm{kN}$, as predicted by quasi-statics. This quasi-static lateral force corresponds to a quasi-static derailment quotient of 0.05 (see Figure 4a), while the derailment quotient from the simulation is 0.11 (see Figure 4b). When the braking takes effect, the lateral force increases on both wheels but more on the rear wheel. Because the vehicle loses speed, the centripetal force decreases, and so does the lateral force on the wheels. The maximum simulated lateral force is $29.5\,\mathrm{kN}$ for the train with buffer-and-chain couplers and $27.5\,\mathrm{kN}$ with Scharfenberg couplers, whereas the quasi-static approach predicted $16.7\,\mathrm{kN}$. This difference from the quasi-static approach is partly because the front wheel transfers most of the load and partly due to dynamic effects. The difference in the lateral force between the two types of couplers is small, approximately 7.3%. The maximum derailment quotient in the case of braking is 0.09 from the quasi-statics and 0.195 from the dynamic simulations. From Figure 7a it can be concluded that the simulated dynamic derailment quotient is not higher than 2 times the quasi-static derailment quotient. This dynamic multiplication factor may be used to make a conservative estimate of the derailment quotient based on quasi-statics.

As the vehicles steadily curve the eigenmode that will be most excited, when braking starts is the longitudinal vibration of the carbodies. One can observe this eigenmode as a standing longitudinal wave in the train. The oscillation in Figure 6b has resonance frequencies at approximately $2.4\,\mathrm{Hz}$, $4.7\,\mathrm{Hz}$, $6.8\,\mathrm{Hz}$ and $8.7\,\mathrm{Hz}$, which is close to the longitudinal eigenmodes (see Table 1). A second eigenmode that is excited is the vehicles' pitch mode. The eigenmode analysis predicts its eigenfrequency at $1.1\,\mathrm{Hz}$, and indeed, in the simulation an oscillation at $1.1\,\mathrm{Hz}$ can be observed.

3.3.2 Derailment quotient when entering a turnout

When a train brakes upon entering the turnout, lateral (roll, yaw, sway) as well as longitudinal modes are excited in the coupling. The eigenfrequencies corresponding to these modes are close to one another (see Table 1), therefore it is not possible to identify these eigenmodes in the frequency domain as could be done in the case of braking while steadily curving.

Figure 8 shows the lateral force on the outer wheels of the leading bogie of the locomotive when entering a 1:9 turnout at $40\,\mathrm{km/h}$. When the wheels enter the turnout the contact on the outer wheel changes from one point contact to two-point contact: one at the wheel flange and one at the wheel tread. When the wheel flange makes contact with the rail there is an impact force. This impact force is important when considering wheel-rail wear or impact

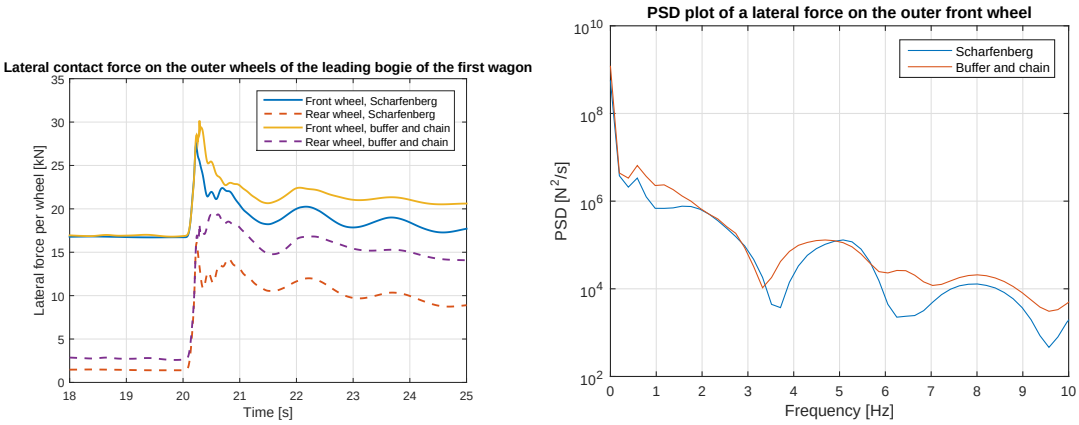

(a) (b)

Figure 6 The lateral force on the outer wheels of the leading bogie of the first wagon in curve at $40\,\mathrm{km/h}$. The vehicle is dynamically simulated steadily curving in a $260\,\mathrm{m}$ radius curve. At time $20\,\mathrm{s}$ the locomotive starts braking with a braking coefficient of 0.4.

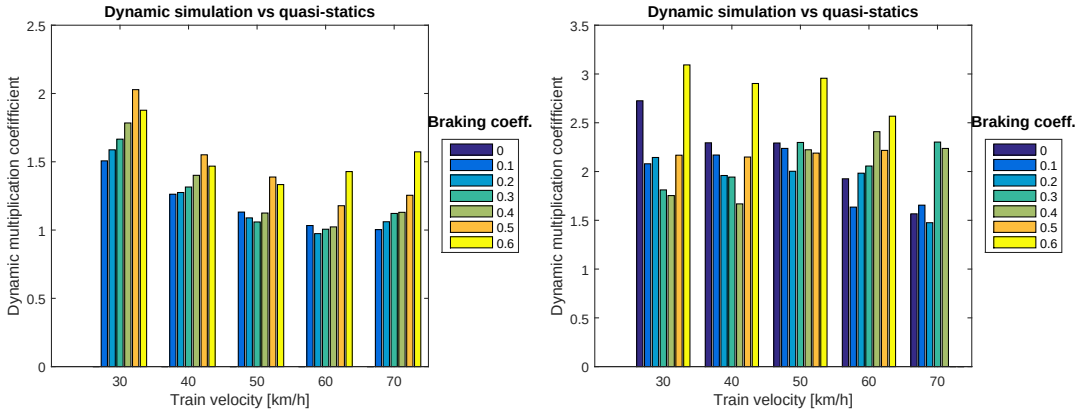

(a) (b)

Figure 7 The dynamic multiplication coefficients, i.e. the ratio between the Y/Q ratios of from the dynamic simulation and from the quasi-static calculations; (a) for the curve, and (b) for the turnout.

noise. However, if the goal is to assess the derailment risk, peak forces lasting less than $50\,\mathrm{ms}$ can be ignored [1]. This $50\,\mathrm{ms}$ threshold was used to create Figure 5b.

The derailment quotients are compared with a threshold as defined by Nadal's criterion (horizontal line in Figure 5b). In this case the criterion was calculated using a friction coefficient of 0.6, corresponding to dry conditions and a wheel flange angle of $65°$, corresponding to a worn wheel profile. At $70\,\mathrm{km/h}$ not all simulations converged due to the high lateral forces so that derailment occurred. Several assumptions made in vehicle simulations do not hold at these high derailment quotients, especially the assumptions made for the wheel-rail contact calculations, such as planar contact and low spin creepage. Because the

assumptions made in the simulation are violated, it is possible that some combinations of vehicle speed and braking converge in the simulation while in reality they would lead to derailment. Indeed, some simulations resulted in a derailment quotient higher than Nadal's maximum, such as all cases with a braking coefficient of 0.6 (irrespective of the speed) and braking coefficients of 0.4 and 0.5 at speeds higher than $70\,\mathrm{km/h}$.

When the first wagon enters the turnout the locomotive starts braking. The dynamic effects of entering the turnout and the application of braking are combined. Entering a curve gives a sudden change in the lateral acceleration. Therefore, the lateral carbody modes are excited: the carbody sway, roll and yaw modes. They cause extra lateral force on the wheels; the maximum lateral force when applying braking after steadily curving is $29.5\,\mathrm{kN}$, while the maximum lateral force when braking (with braking coefficient of 0.4) upon entrance to the turnout is $48.4\,\mathrm{kN}$, ignoring peaks in the force shorter than $50\,\mathrm{ms}$. These lateral forces correspond to a derailment quotient of 0.20 without braking and 0.41 with braking (see Figure 5b). In the quasi-static calculations shown in Figure 5a these derailment quotients are, respectively, 0.085 and 0.23, which means that taking account of the dynamics increases the lateral force by 135% for a train coasting through the turnout and by 78% for braking with a braking coefficient of 0.4. Another observation is that the quasi-static derailment quotient in Figure 5a changes linearly with the braking coefficient. For the dynamic simulations, the increase in derailment quotient is irregular, though generally faster than linear with the braking coefficient. In fact, in the case of a braking coefficient of 0.6, the Nadal criterion is always exceeded even at low speed. From Figure 7b we can conclude that the derailment quotient from simulation is at most 3 times larger than the derailment quotient estimated from quasi-statics. So a dynamic multiplication coefficient of 3.1 can be used to obtain a conservative estimate of the dynamic derailment coefficient once the quasi static derailment coefficient has been calculated.

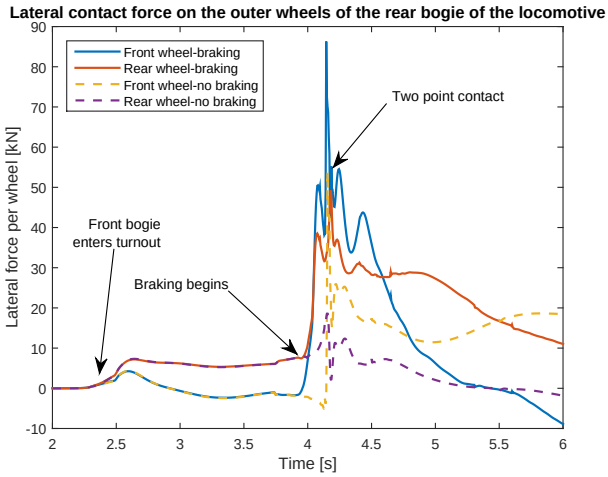

Figure 8 The lateral force on the outer wheels of the rear bogie of the locomotive when entering a 1:9 turnout obtained through vehicle dynamic simulation. Just before the rear bogie of the locomotive enters the turnout, the locomotive starts braking with a braking coefficient of 0.4.

4 Discussion and further research

Seventy (2x5x7) vehicle simulations have been performed through a curve and a turnout, each with 5 different vehicle speeds and 7 different braking coefficients. Each simulation resulted in a maximum derailment quotient, that can be compared with the results from quasi-static calculatio to determine a dynamic multiplication coefficient. For braking while curving, the dynamic multiplication coefficient is 2.5, whereas for braking in a turnout the dynamic multiplication coefficient is 2.2. Moreover, in a turnout braking coefficients higher than 0.5 result in derailment irrespective of the vehicle speed. A conservative approach would be to adhere to a dynamic multiplication coefficient of 2.5 for all cases, while limiting the braking coefficient to 0.5. This outcome does not mean that a higher braking coefficient cannot be achieved, only that it should not be applied by the leading locomotive in a turnout. In an emergency situation the braking is usually applied all the wheels of a train, however attention needs to be paid to the timing with which the different braking systems are applied. Future research is needed to determine these dynamic multiplication coefficients for different turnouts, different curve radii and different train configurations. An experimental validation of the proposed approach can be achieved by measuring the Y/Q ratio by instrumented wheelsets or by measuring the displacement in the primary suspension [26]. The measures can then be used to validate the vehicle/train model. The determination of the dynamic multiplication coefficients would still needs to be obtained through vehicle dynamic simulations with a validated vehicle. This is because the determination of the dynamic multiplication coefficient would require a vast number of simulations (different speeds, train composition, traction/braking effort), which would not be practically possible with measurements.

The case of braking is relevant for the scenario of a train entering a turnout at a speed higher than allowed and trying to correct that by strong braking. Because this is potentially a dangerous scenario, this article has chosen the braking scenario to show the methodology; however, the same methodology can be used for a trailing locomotive that initiates traction (acceleration). This scenario also results in compressive coupler forces and subsequently increased lateral forces from between wheel and rail. The quasi-static analysis would result in the same forces at the most loaded coupler, which in this case is the coupler between the locomotive and the last of the wagons.

The lateral forces originating from centripetal forces or from the lateral coupler forces can cause derailment, but also vehicle rollover due to wheel unloading. The common criterion for wheel unloading is that the vertical dynamic force on one wheel should be at least 60% of the normal wheel load (half the axle load). For a fast estimate of this vertical dynamic load the same methodology could be used as for the derailment coefficient in this article: making use of the moments cause by the centripetal force and lateral coupler force a quasi static vertical force can be calculated. This quasi-static vertical force can then be compared to dynamic vertical forces obtained through dynamic vehicle simulation to obtain a dynamic multiplication coefficient that is valid in a sufficiently large range of vehicle speed and traction/braking effort. Similarly as for the derailment coefficient it will be necessary to define a different dynamic multiplication coefficient for the case of a turnout (no transition curve) and for normal curves.

The train model here was of a passenger train consisting of a locomotive and 7 wagons; however, our methodology and the estimation/mapping method could be extended to long freight trains and provide a tool for heavy haul operators. Using a full model for each vehicle would generate a large number of degree of freedom in long trains and corresponding

calculation time. This drawback can be avoided using the approach of [11]: a long train modeled with one degree of freedom per vehicle, with only the vehicles of interest are modeled in detail.

5 Conclusions

We propose a methodology to assess the increase in derailment risk due to pushing or braking a train through an estimate of the derailment quotient obtained by multiplying a derailment quotient calculated from quasi-statics by a dynamic multiplication coefficient. These derailment quotients can be compared to the Nadal criterion to assess the derailment risk. Based on vehicle dynamic simulations, the dynamic multiplication coefficient is estimated as 2 in curves and 3.1 in turnouts.

The derailment quotient has been mapped as function of speed and braking or traction (as a braking coefficient or as a total braking force). These maps are easy to interpret and do not require deep knowledge of the train dynamics; accordingly, they can be used by operators to determine a braking/traction strategy, either automated in a control system, or as guidelines to drivers. Two different couplers were considered: one transferring only force in the coupler direction and one that also transfers moment between the carbodies. The effect of the type of couplers on the lateral wheel-rail force was found to be small, approximately $8\,\%$.

References

[1] C. Cole. Longitudinal train dynamics. In Simon Iwnicki, editor, *Handbook of Railway Vehicle Dynamics*, pages 239–278. Taylor and Francis, Boca Raton, FL, USA, 2006.

[2] C. Cole and Y.Q. Sun. Simulated comparisons of wagon coupler systems in heavy haul trains. *Proceedings of the Institution of Mechanical Engineers, Part F: Journal of Rail and Rapid Transit*, 220:247–256, 2006.

[3] Vijay Kumar Garg and Rao V. Dukkipati. *Dynamics of railway vehicle systems*. Academic Press, London, UK, 1984.

[4] T. Geike. Understanding high coupler forces at metro vehicles. *Vehicle System Dynamics*, 45:389–396, 2007.

[5] Saeed Mohammadi and Asghar Nasr. Effects of power unit location on in-tain longitudinal forces during brake application. *Int. J. of Vehicle Systems Modelling and Testing*, 5:176–196, 2010.

[6] M. Anseri, E. Esmailzadeh, and D. Younesian. Longitudinal dynamics of freight trains. *Int. J. of Heavy Vehicle Systems*, 16:102–131, 2009.

[7] M. McClanachan, C. Cole, D. Roach, and B. Scown. An investigation of the effect of bogie and wagon pitch associated with longitudinal train dynamics. *Vehicle System Dynamics*, 33:374–385, 2000.

[8] M. El-Sibaie. Recent advancements in buff and draft testing techniques. In *Proceedings of the IEEE/ASME joint railroad conference, Pittsburgh, PA, USA*, pages 115–119, 1993.

[9] C. Cole, M. Maksym Spiryagin, and Y. Q. Sun. Assessing wagon stability in complex train systems. *International Journal of Rail Transportation*, 1:193–217, 2013.

[10] S. Simson. *Three axle locomotive bogie steering, simulation of powered curving performance passive and active steering bogies*. PhD thesis, Central Queensland University, 2009.

[11] Z.Q. Xu, W.H. Ma, Q.Wu, and S.H. Luo. Coupler rotation behaviour and its effect on heavy haul trains. *Vehicle System Dynamics*, 51:1919–1838, 2013.

[12] Ziquang Xu, W.H. Ma, Q.Wu, and S.H. Luo. Analysis of the rotation angle of a coupler used on heavy haul locomotives. *Proceedings of the Institution of Mechanical Engineers, Part F: Journal of Rail and Rapid Transit*, 228:835–844, 2013.

[13] R. Menssen and W. Kik. Running through a switch - simulation and test. *Vehicle System Dynamics*, 23:378–389, 1994.

[14] E. Kassa and J.C.O. Nielssen. Dynamic train-turout interaction in an extended frequency range using a detailed model of track dynamics. *Journal of Sound and Vibration*, 320:893–914, 2009.

[15] S. Alfi and S. Bruni. Mathematical modeling of train-turnout interaction. *Vehicle System Dynamics*, 47:551–574, 2009.

[16] M. Wiest, E. Kassa, W. Daves, and J.C.O. Nielsen. Assessment of methods for calculating contact pressure in wheel-rail/switch contact. *Wear*, 265:1439–1445, 2008.

[17] X. Shu, N. Nilson, C. Sasaoka, and J. Elkins. Development of a real-time wheel/rail contact model in nucars and apllication to diamond crossing and turnout design simulations. *Vehicle System Dynamics*, 44:251–260, 2006.

[18] Nico Burgelman, Zili Li, and Rolf Dollevoet. A new rolling contact method applied to conformal contact and the train-turnout interaction. *Wear*, 321:94–105, 2014.

[19] C. Esveld. *Modern Railway Track*. MRT-productions, Dordrecht, Netherlands, 2010.

[20] Office for Research and Experiments of the International Union of Railways. Dynamic vehicle/track interaction phenomena from the point of track maintenance. Technical Report ORE D161 rp3, 1987.

[21] S. Jovanovic and C. Esveld. Ecotrack: an objective condition-based decision support system for long-term track m&r planning directed towards the reduction of life cycle costs. In *7th international Heavy Haul conference, Brisbane, Australia*, pages 199–207, 2001.

[22] S. L. Grassie. Models of railway track and vehicle/track interaction at high frequencies: Results of benchmark test. *Vehicle System Dynamics*, 25:243–262, 1996.

[23] B. Dietrichs, M. Ekequist, S. Stichel, and H. Tengstrand. Quasi-static modelling of wheel-rail contact reactions due to crosswind effects for various types of high speed rolling stock. *Proceedings of the Institution of Mechanical Engineers, Part F: Journal of Rail and Rapid Transit*, 218:133–148, 2004.

[24] B. Dirks and P. Wiersma. Meting railprofiel tongbeweging van wissels 105a en 271 te eindhoven. Technical report, DeltaRail, 2007.

[25] O. Arias-Cuevas, Z. Li, and C. Esveld. Simulation of the lateral dynamics of a railway vehicle and its validation based on rail wear measurements. In *Proceedings of the ECCOMAS Thematic Conference on Multibody, Milan, Italy*, pages 1–10, 2007.

[26] A. Matsumoto, Y. Sato, H. Ohno, M. Shimizu, J. Kurihara, T. Saitou, Y. Michitsuji, R. Matsui, M Tanimoto, and M Mizuno. Actual states of wheel/rail contact forces and friction on sharp curves - continuous monitoring from in-service trains and numerical simulations. *Wear*, 314:189–197, 2014.